Available online at www.sciencedirect.com

ScienceDirect

Mendeleev Commun., 2021, **31**, 415–418

Mendeleev Communications

Solid-state reaction of niobium with diamond carbon at high pressure and high temperature to form superconducting composite

Vladimir Yu. Osipov,*[a,b] Fedor M. Shakhov,[a] Nikolai M. Romanov[c,d] and Kazuyuki Takai[b]

[a] *Ioffe Institute, Russian Academy of Sciences, 194021 St. Petersburg, Russian Federation. Fax: +7 812 297 1017; e-mail: osipov@mail.ioffe.ru*
[b] *Department of Chemical Science and Technology, Hosei University, Koganei, 184-8584 Tokyo, Japan*
[c] *School of Engineering Science, LUT University, 53850 Lappeenranta, Finland*
[d] *Joint-Stock Company 'Svetlana-Semiconductors', 194156 St. Petersburg, Russian Federation*

DOI: 10.1016/j.mencom.2021.05.044

Niobium carbide composites were obtained by sintering niobium powder and detonation nanodiamond at high pressure (7 GPa) and high temperature (~1990 °C) for several tens of seconds. The resulting composites demonstrate a set of distinct reflections from the NbC phase in the X-ray diffraction pattern and exhibit superconducting properties at temperatures below 11.4 K.

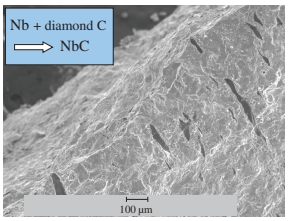

SEM image of the prepared NbC composite with the remaining carbon inclusions

Keywords: niobium, detonation nanodiamond, sintering at high pressure, superconducting composite, electron microscopy, X-ray diffraction, magnetochemistry, magnetic studies.

Detonation nanodiamonds (DNDs) with an average size of about 5 nm are a modern precursor material in the global market, which finds extensive technological applications.[1–3] DNDs and their surface-modified derivatives have been widely discussed in the literature over the past two decades regarding the diamond surface chemistry and grafted foreign molecules and ligands' characteristics.[4–7] DNDs are promising research objects not only as biologically inert nanoscale platforms for grafting various atomic groups and long-chain molecules but also as a material for creating various diamond-reinforced hard metal composites. In addition to two-phase composites, in which the carbon and metal phases retain their individuality at the nanoscale, composites in which these phases form carbides with high thermal resistance are of great interest. In this case, solid-phase chemical reactions occurring at high temperatures, when diffusion is significant, are responsible for the formation of new phases.[8,9] Note that, besides the reaction between solid reactants, carbides can also form when one reactant is in the gaseous phase. For example, this is the case of high-temperature (~1600 °C) diffusion of carbon from methane into a niobium wire.[10] For the production of metal carbides, particularly niobium carbide, precursors of carbon, such as fullerenes, nanotubes and other forms of carbon, have been mainly used in the last three decades, but very rarely DNDs.[11–14,†] This is because diamond is difficult to force to react since, for effective sintering with metal, it must first go into the sp^2-carbon state and further react with the metal to form carbide. Niobium and niobium carbide are materials of great technological importance.[15–17] They can be used to create various modern advanced electronic and magnetoelectronic vortex-based devices, sensors and energy storage devices and improve the mechanical properties of many structural materials.[18–21] Transition metal carbides exhibit their inherent chemical reactivity, as do the elements further to the right in the Periodic Table, and can be catalysts and electrocatalysts for some practically significant reactions.[22–24]

Although the synthesis of niobium carbide from diamond carbon and niobium has been reported,[25,26] the resulting composites have not been characterized by elemental analysis, X-ray diffraction and electron microscopy. In this work, we carried out the reaction of niobium with DND carbon by rapid sintering at high pressure and high temperature (HPHT) and characterized the resulting composite by various methods. For simplicity, we ignored the role of the surface of DND particles coated with various oxygen-containing functional groups and bearing foreign atoms but considered the participation of DND internal carbon atoms in forming new carbide compounds.

We used commercially available highly purified (ash content < 0.1 wt%) DNDs and pure (99.9%) niobium powder with a grain size of 45 μm (see Online Supplementary Materials). The size of DND aggregates consisting of diamond crystallites 5 nm in size was ~100–200 nm. According to X-ray photoelectron spectroscopy data, the surface oxygen content in the precursor DND was 8.2 at%.[27] This oxygen is contained in various functional groups (mainly carboxyl, hydroxyl and anhydride) on the surface of a nanodiamond particle and inside loose DND aggregates.[28–30] We assume that some of the primary particles in an aggregate are linked by anhydride groups containing C–O and C–O–C bonds.

We prepared Nb/DND mixtures of various compositions with an Nb/C weight ratio of 100:0 (1), 80:20 (2) and 90:10 (3). The prepared Nb/DND mixture was then transferred into a hollow graphite cylinder (4.0 mm inner diameter, 5.5 mm high) with two graphite lids inside a toroidal-type high-pressure chamber for sintering. Thus, in one pressing cycle, it was possible to process about ~250 mg of precursor Nb/DND mixture. Then, sintering

† Following Fukunaga *et al.*,[14] niobium carbides can be prepared by powder metallurgy at 1300–1400 °C and iodine-assisted solid-state reaction using carbon nanotubes during heat treatment at 1000–1100 °C.

© 2021 Mendeleev Communications. Published by ELSEVIER B.V. on behalf of the N. D. Zelinsky Institute of Organic Chemistry of the Russian Academy of Sciences.

took place at high pressure (7 GPa) and high temperatures (from 1330 to 1990 °C) for 60 s in such a press with a toroidal chamber. A schematic of the high-pressure chamber was previously published.[31]. The components of sample Nb26 (composition 3) were sintered at the maximum possible temperature of 1990 °C, which is lower than the melting point of niobium at normal pressure (2470 °C). Since the molar masses of niobium and niobium carbide are 92.91 and 104.92 g mol^{-1}, respectively, a mixture with a stoichiometric ratio of precursor components should contain 88.6 wt% Nb and 11.4 wt% C. Composites, sintered from a mixture of composition 2 with a large excess of carbon, turned out not interesting for fundamental research and are not considered further. Nevertheless, an excess of carbon in mixture 2 does not interfere with the sintering of solid tablets; they retain the shape given by the high-pressure cell and do not disintegrate, although they become brittle.

For composition 3, there is the following deviation from stoichiometry: an excess of niobium (+1.4%) and a lack of carbon (–1.4%). In practice, in our case, a slight lack of carbon must be compensated for by the reaction of niobium with the graphite container's carbon. Note that Nb/DND composition 3, which we mainly used in this work, is very close to stoichiometric. The samples removed from the high-pressure cell after sintering had a diameter and height of ~4.0 and ~2.5 mm, respectively. The actual weight of the dense NbC pellets synthesized from composition 3 ranged from 230 to 236 mg.

An image of a sintered composite Nb26 broken in half is shown in Figure S1. The fracture surface has a pronounced metallic luster, in contrast to the dark side surfaces in contact with the graphite chamber. Scanning electron microscopy (SEM) was used to analyze the lateral fracture of composite Nb26. Two SEM images of sample Nb26, along with the results of energy-dispersive X-ray spectroscopy (EDS) analysis of some selected species, are presented in Figure 1 and Table 1. Separate elongated carbon inclusions are visible on the fracture surface, oriented mainly perpendicular to the press compression axis. Their presence means that some of the carbon did not react with niobium. This carbon probably forms an independent phase after removing the load and pressure in local regions oversaturated with carbon. The elemental composition of the fracture surface in the regions marked by rectangles 1–5 is given in Table 1.

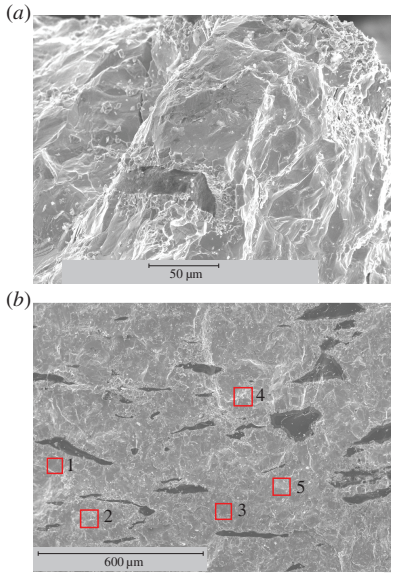

Figure 1 SEM images of two selected species of small and large areas found on a transverse fracture of sample Nb26 at (*a*) higher and (*b*) lower magnifications. SEM EDX elemental analysis data for squares 1–5 are given in Table 1. Accelerating voltage 20 kV. Magnification 500 x (top panel).

Table 1 Elemental composition of selected surface areas on a transverse fracture of sample Nb26, measured by SEM EDS.

Surface area[a]	Element content (wt%)			
	C	O	Nb	Total
1	13.17	1.64	85.19	100.00
2	13.87	3.22	82.92	100.00
3	14.74	1.23	84.03	100.00
4	16.47	2.68	80.85	100.00
5	9.67	3.04	87.29	100.00

[a] For numbers of surface areas, see Figure 1(*b*).

Although the elemental composition of these regions is close to stoichiometric, there is an excess of carbon and even oxygen in them. Oxygen probably appears due to surface oxidation with atmospheric oxygen (after synthesis) or oxygen of the surface groups of DND particles (during synthesis). According to EDS analysis, the excess carbon in selected regions 1–4 is about 3.2 wt% compared to the stoichiometric value of 11.4 wt%.

Mo Kα X-ray diffraction patterns (see Online Supplementary Materials) of niobium powder and sample Nb26 are shown in Figure 2. Intense reflections from planes 111, 200, 220, 311, 222, 400, 331 and 420 of the NbC phase are visible on the XRD pattern of sample Nb26 (curve *1*). Such a family of reflections, which is a reliable proof of the presence of the NbC phase, was noted in several works, but mainly for Cu Kα X-ray radiation.[21,32–35] Besides, this XRD pattern contains several much less intense peaks of the niobium phase. Five narrow peaks assigned to reflections from planes 110, 200, 211, 220 and 310 of the precursor niobium powder (grain size of 45 μm) are shown in Figure 2 (curve *2*) for comparison and identification of the remaining Nb phase in sample Nb26. Broadened reflections in the XRD pattern of sample Nb26 indicate that this composite consists of cemented NbC and Nb grains 1 μm or less. Some well-faceted crystallites of NbC, Nb or both are visible in high-resolution SEM images (Figure S2). Since the composite contains a pure niobium phase according to XRD data, the carbon phase should also be present in the same atomic content. The latter is observed in SEM micrographs of sample Nb26 in the form of black inclusions (see Figure 1). Thus, we can assume that this composite has the composition NbC–Nb–C, in which the atomic ratio Nb/C ≈1.16 and the mass of unreacted niobium

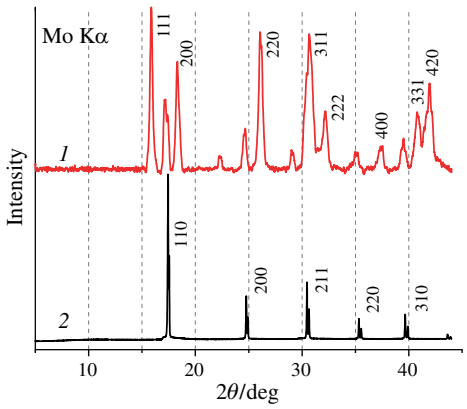

Figure 2 Powder XRD patterns of (*1*) composite Nb26 sintered under high pressure and (*2*) precursor niobium powder with a grain size of ~45 μm or less, obtained using Mo Kα radiation (λ = 0.7093 Å). Diffractogram *1* clearly shows eight reflections related to the cubic phase of NbC with the space group *Fm*-3*m* (no. 225) and the unit cell parameter a = 4.4691 Å. No peaks associated with NbO and diamond were found in diffractogram *1*. The peaks at 22.3 and 29.1° were not identified.

is no less than 15–20 wt%, based on the mass of the formed NbC phase.

The resulting material was investigated using SQUID magnetometry (see Online Supplementary Materials) for superconductivity different from that of pure niobium. The temperature dependence of the magnetic susceptibility of sample Nb26 is shown in Figure 3. The magnetic susceptibility is positive at $T > 12$ K and is approximately equal to $+6.6 \times 10^{-7}$ emu Oe^{-1} g^{-1} at 12–100 K. This interval corresponds to the normal metal state of composite Nb26. In the temperature range of 12–300 K, we did not find a corresponding noticeable contribution to the Nb26 susceptibility from the Curie-type paramagnetism of DND,[29,30] which could hypothetically remain from DNDs added to the composite mixture in an amount of ~23 mg if it had not been subjected to graphitization and solid-phase reaction. This result means that almost all DNDs were both consumed during the high-temperature solid-phase reaction and partially graphitized.

With decreasing temperature, the magnetic susceptibility changes from positive to negative values in the vicinity of 11.4 K [Figure 3(*b*)], then falls almost abruptly in the region below 5 K, gradually approaching a constant negative value of $\chi_0 = -3.73 \times 10^{-3}$ emu Oe^{-1} g^{-1} at temperatures below 3.5 K [Figure 3(*a*)]. This χ_0 value with an accuracy of 35% is close to that found earlier[32] for the NbC/C nanocomposite containing NbC nanocrystals ~10 nm in size. The temperature at which the magnetic susceptibility changes sign is the transition temperature to the superconducting state with moderate diamagnetism. In this case, numerous superconducting regions appear in the composite, isolated or connected in percolation paths. Thus, in composite Nb26 under study, the transition to superconductivity occurs at $T_c = 11.4$ K. In the temperature range 2–5 K, the sample demonstrates a highly developed superconducting state with extremely high diamagnetism. The value of 11.4 K corresponds to the superconducting transition temperature in near-stoichiometric niobium carbide species.‡ The substantial drop in susceptibility in the region below 5 K is mainly because part of the material is in the nonstoichiometric state NbC_{1-x}, where x is between 0.15 and 0.2, or contains unreacted niobium. Thus, the magnetic susceptibility data indirectly indicates the successful synthesis of the NbC phase in composite Nb26, although some remaining species of niobium and graphite are still present in the composite. Incidentally, the lower critical field (H_{c1}) and upper critical field (H_{c2}) measured at 2 K are ~300 and ~8900 Oe, respectively (Figure S3), which are very close to the corresponding values for niobium carbide synthesized by other direct methods, including the solid-state reaction for growing single-crystal NbC.[12,19]

In conclusion, although the synthesis of niobium carbide from various carbon and niobium-containing powder precursors has been well known for a long time, we have implemented its direct synthesis by rapid sintering (50–60 s) of nanodiamond carbon and pure niobium powder under HPHT conditions. The best quality and morphology of NbC composites were found for the selected material, prepared from a near stoichiometric Nb/DND mixture at a sintering temperature of 1990 °C. The practical advantages of using DND instead of the sp^2 forms of carbon are worthy of note. The bulk density of DND powder is higher than that of any sp^2-hybridized nanocarbon. It forms denser mixtures with metal powder and does not 'stick together' into flakes during grinding, like multilayer graphene or nanographite. As a result, the mixture of powdered niobium with DND is more homogenized and dense than with the sp^2 forms of carbon. This advantage is especially pronounced in the graphitization of diamond under HPHT conditions when the net volume occupied by carbon increases and the compact becomes denser due to 'self-expansion' from inside and fewer voids at the nanoscale.

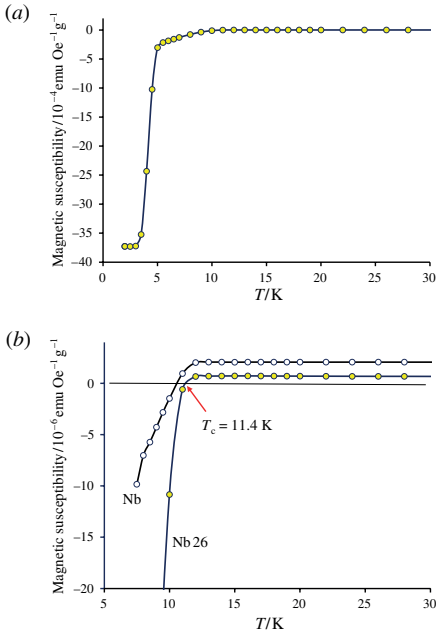

Figure 3 (*a*) The temperature dependence of the magnetic susceptibility of sample Nb26 measured in a magnetic field of 250 Oe and (*b*) its comparison with the analogous dependence of a pure niobium tablet pressed at 7 GPa and 1820 °C. The data were obtained in a slow heating mode from 2 to 300 K. Data above 30 K are not shown for simplicity. Cooling to a temperature of 2 K was carried out in a zero magnetic field. The temperature range below 11.4 K corresponds to the diamagnetic superconducting state of sample Nb26 with negative magnetic susceptibility. Sample weight was ~232 mg.

The resulting composites exhibit good superconducting properties with a superconducting transition temperature of about 11.4 K. This approach paves the way for the rapid fabrication of niobium carbide parts for some special purposes, such as electrodes for carbon plasma emission. The presence of carbon and niobium inclusions in the fabricated composites with NbC should not significantly affect superconductivity characteristics since the NbC phase content prevails.

F.S. thanks the Ioffe Institute for support (project no. 0040-2014-0013), and V.O. thanks the Japan Society for the Promotion of Science and Hosei University for their support (JSPS Fellowship no. L17526). K.T. acknowledges the support of JSPS KAKENHI (grant nos. 16K05758, 19K05410 and 26107532).

Online Supplementary Materials

Supplementary data associated with this paper can be found in the online version at doi: 10.1016/j.mencom.2021.05.044.

References

1 *Detonation Nanodiamonds: Science and Applications*, eds. A. Ya. Vul' and O. A. Shenderova, Pan Stanford, Singapore, 2014.
2 *Nanodiamonds: Advanced Material Analysis, Properties and Applications*, ed. J.-C. Arnault, Elsevier, Amsterdam, 2017.
3 V. Yu. Dolmatov, A. N. Ozerin, I. I. Kulakova, O. O. Bochechka, N. M. Lapchuk, V. Myllymäki and A. Vehanen, *Russ. Chem. Rev.*, 2020, **89**, 1428.
4 A. Krueger, in *Nanodiamond* (Nanoscience series), ed. O. A. Williams, Royal Society of Chemistry, Cambridge, 2014, pp. 49–88.

‡ For niobium, the superconducting transition temperature is 9.25 K. For nonstoichiometric niobium carbides with the composition NbC_{1-x} (x = = 0.03–0.19), the T_c value is usually several degrees less than 11 K (in the range down to $T_c \approx 3$ K for $x = 0.19$) depending on the ordered or disordered state of the material.[16]

5 V. Yu. Osipov, D. W. Boukhvalov and K. Takai, *Mendeleev Commun.*, 2020, **30**, 436.
6 V. Yu. Osipov, D. W. Boukhvalov and K. Takai, *Mendeleev Commun.*, 2019, **29**, 452.
7 V. Yu. Osipov, N. M. Romanov, K. Kogane, H. Touhara, Y. Hattori and K. Takai, *Mendeleev Commun.*, 2020, **30**, 84.
8 Yu. D. Tret'yakov, *Tverdofaznye Reaktsii* (*Solid-Phase Reactions*), Khimiya, Moscow, 1978 (in Russian).
9 V. V. Gusarov, *Russ. J. Gen. Chem.*, 1997, **67**, 1846 (*Zh. Obshch. Khim.*, 1997, **67**, 1959).
10 K.-H. Bernhardt, *Z. Naturforsch., A: Phys., Phys. Chem., Kosmophys.*, 1975, **30**, 528.
11 M. Scheffler, O. Dernovsek, D. Schwarze, A. H. A. Bressiani, J. C. Bressiani, W. Acchar and P. Greil, *J. Mater. Sci.*, 2003, **38**, 4925.
12 R. Jha and V. P. S. Awana, *J. Supercond. Novel Magn.*, 2012, **25**, 1421.
13 H. X. Geng, G. C. Che, W. W. Huang, S. L. Jia, H. Chen and Z. X. Zhao, *Supercond. Sci. Technol.*, 2007, **20**, 211.
14 A. Fukunaga, S. Chu and M. E. McHenry, *J. Mater. Sci. Lett.*, 1999, **18**, 431.
15 M. G. D. V. Cuppari and S. F. Santos, *Metals*, 2016, **6**, 250.
16 A. A. Rempel', *Phys.-Usp.*, 1996, **39**, 31 (*Usp. Fiz. Nauk*, 1996, **166**, 33).
17 *The Chemistry of Transition Metal Carbides and Nitrides*, ed. S. T. Oyama, Springer, Dordrecht, 2012.
18 O. V. Dobrovolskiy, D. Yu. Vodolazov, F. Porrati, R. Sachser, V. M. Bevz, M. Yu. Mikhailov, A. V. Chumak and M. Huth, *Nat. Commun*., 2020, **11**, 3291.
19 D. Yan, D. Geng, Q. Gao, Z. Cui, C. Yi, Y. Feng, C. Song, H. Luo, M. Yang, M. Arita, S. Kumar, E. F. Schwier, K. Shimada, L. Zhao, K. Wu, H. Weng, L. Chen, X. J. Zhou, Z. Wang, Y. Shi and B. Feng, *Phys. Rev. B*, 2020, **102**, 205117.
20 A. Tolosa, B. Krüner, S. Fleischmann, N. Jäckel, M. Zeiger, M. Aslan, I. Grobelsek and V. Presser, *J. Mater. Chem. A*, 2016, **4**, 16003.
21 R. Magalhães Triani, F. Edson Mariani, L. Fuscaldi De Assis Gomes, P. G. Bonella De Oliveira, G. E. Totten and L. C. Casteletti, *Lubricants*, 2019, **7**, 63.
22 S. T. Oyama, *J. Solid State Chem.*, 1992, **96**, 442.
23 S. T. Oyama, *Catal. Today*, 1992, **15**, 179.
24 W.-F. Chen, J. T. Muckerman and E. Fujita, *Chem. Commun.*, 2013, **49**, 8896.
25 G. A. Dubitskiy, V. D. Blank, S. G. Buga, E. E. Semenova, V. A. Kul'bachinskii, A. V. Krechetov and V. G. Kytin, *JETP Lett.*, 2005, **81**, 260 (*Pis'ma Zh. Eksp. Teor. Fiz.*, 2005, **81**, 323).
26 G. A. Dubitsky, V. D. Blank, S. G. Buga, E. E. Semenova, N. R. Serebryanaya, V. V. Aksenenkov, V. M. Prokhorov, V. A. Kul'bachinski, A. V. Krechetov and V. G. Kytin, *Z. Naturforsch., B: J. Chem. Sci.*, 2006, **61**, 1541.
27 V. Yu. Osipov, N. M. Romanov, F. M. Shakhov and K. Takai, *J. Opt. Technol.*, 2018, **85**, 122.
28 V. Yu. Osipov, A. E. Aleksenskiy, A. I. Shames, A. M. Panich, M. S. Shestakov and A. Ya. Vul', *Diamond Relat. Mater.*, 2011, **20**, 1234.
29 I. D. Gridnev, V. Yu. Osipov, A. E. Aleksenskii, A. Ya. Vul' and T. Enoki, *Bull. Chem. Soc. Jpn.*, 2014, **87**, 693.
30 V. Yu. Osipov, N. M. Romanov and K. Takai, *Mendeleev Commun.*, 2021, **31**, 227.
31 F. M. Shakhov, A. M. Abyzov and K. Takai, *J. Solid State Chem.*, 2017, **256**, 72.
32 D. Li, W. F. Li, S. Ma and Z. D. Zhang, *Phys. Rev. B*, 2006, **73**, 193402.
33 A. Gupta, M. Mittal, M. K. Singh, S. L. Suib and O. P. Pandey, *Sci. Rep.*, 2018, **8**, 13597.
34 C. Ang, L. Snead and K. Benensky, *Int. J. Ceram. Eng. Sci.*, 2019, **1**, 92.
35 X. Zhao, M. Togaru, Q. Guo, C. R. Weinberger, L. Lamberson and G. B. Thompson, *J. Eur. Ceram. Soc.*, 2019, **39**, 5167.

Received: 5th February 2021; Com. 21/6443